

Adversarial Permutation Guided Node Representations for Link Prediction

Indradymna Roy, Abir De, Soumen Chakrabarti

Indian Institute of Technology Bombay
 {indraroy15, abir, soumen}@cse.iitb.ac.in

Abstract

After observing a snapshot of a social network, a link prediction (LP) algorithm identifies node pairs between which new edges will likely materialize in future. Most LP algorithms estimate a score for currently non-neighboring node pairs, and rank them by this score. Recent LP systems compute this score by comparing dense, low dimensional vector representations of nodes. Graph neural networks (GNNs), in particular graph convolutional networks (GCNs), are popular examples. For two nodes to be meaningfully compared, their embeddings should be indifferent to reordering of their neighbors. GNNs typically use simple, symmetric set aggregators to ensure this property, but this design decision has been shown to produce representations with limited expressive power. Sequence encoders are more expressive, but are permutation sensitive by design. Recent efforts to overcome this dilemma turn out to be unsatisfactory for LP tasks. In response, we propose PERMGNN, which aggregates neighbor features using a recurrent, order-sensitive aggregator and directly minimizes an LP loss while it is ‘attacked’ by adversarial generator of neighbor permutations. By design, PERMGNN has more expressive power compared to earlier symmetric aggregators. Next, we devise an optimization framework to map PERMGNN’s node embeddings to a suitable locality-sensitive hash, which speeds up reporting the top- K most likely edges for the LP task. Our experiments on diverse datasets show that PERMGNN outperforms several state-of-the-art link predictors by a significant margin, and can predict the most likely edges fast.

1 Introduction

In the link prediction (LP) task, we are given a snapshot of a social network, and asked to predict future links that are most likely to emerge between nodes. LP has a wide variety of applications, *e.g.*, recommending friends in Facebook, followers in Twitter, products in Amazon, or connections on LinkedIn. An LP algorithm typically considers current non-edges as potential edges, and ranks them by decreasing likelihoods of becoming edges in future.

1.1 Prior work and their limitations

LP methods abound in the literature, and predominantly follow two approaches. The first approach relies strongly on hand-engineering node features and edge likelihoods based on the network structure and domain knowledge [3, 16, 23]. However, such feature engineering often demands significant domain expertise. The second approach learns low dimensional node embeddings which serve as node features in LP tasks. Such embedding models include Node2Vec [12], DeepWalk [31], etc., and various graph neural networks (GNN), *e.g.*, GCN [17], GraphSAGE [13], GAT [43], etc.

Limited expressive power of GNNs. While deep graph representations have shown significant potential in capturing complex relationships between nodes and their neighborhoods, they lack representational power useful for LP. A key reason for this weakness is the use of symmetric aggregates over a node u ’s neighbors, driven by the desideratum that the representation of u should be invariant to a permutation of its neighbor nodes [32, 33, 52]. Such networks have recently been established as low-pass filters [29, 47], which attenuate high frequency signals. This prevents LP methods based on such node representations from reaching their full potential. Although recent efforts [5, 20, 38, 40, 41] on modeling inter-item dependencies have substantially improved the expressiveness of set representations in applications like image and text processing, they offer only modest improvement for LP, as we shall see in our experiments.

Limitations of sequence driven embeddings. We could arrange the neighbors of u in some arbitrary canonical order, and combine their features sequentially using, say, a recurrent neural network (RNN). This would capture feature

correlations between neighbors. But now, the representation of u will become sensitive to the order in which neighbors are presented to the RNN. In our experiments, we see large degradation of LP accuracy when neighbors are shuffled. We seek to resolve this central dilemma. An obvious attempted fix would be to present many permutations (as Monte Carlo samples) of neighbor nodes but, as we shall see, doing so in a data-oblivious manner is very inefficient in terms of space and time.

1.2 Our proposal: PERMGNN

In response to the above limitations in prior work, we develop PERMGNN: a novel node embedding method specifically designed for LP. To avoid the low-pass nature of GNNs, we eschew symmetric additive aggregation over neighbors of a node u , instead using a recurrent network to which neighbor node representations are provided sequentially, in some order. The representation of u is computed by an output layer applied on the RNN states.

To neutralize the order-sensitivity of the RNN, we cast LP as a novel min-max optimization, equivalent to a game between an adversary that generates worst-case neighbor permutations (to maximize LP loss) and a node representation learner that refines node representations (to minimize LP loss) until they become insensitive to neighborhood permutations. To facilitate end-to-end training and thus avoiding exploration of huge combinatorial permutation spaces, the adversarial permutation generator is implemented as a Gumbel-Sinkhorn neural network [26].

Next, we design a hashing method for efficient LP, using the node representation learnt thus far. We propose a smooth optimization to compress the learned embeddings into binary representations, subject to certain hash performance constraints. Then we leverage locality sensitive hashing [11] to assign the bit vectors to buckets, such that nodes likely to become neighbors share buckets. Thus, we can limit the computation of pairwise scores to within buckets. In spite of this additional compression, our hashing mechanism is accurate and fast.

We evaluate PERMGNN on several real-world datasets, which shows that our embeddings can suitably distill information from node neighborhoods into compact vectors, and offers substantial accuracy boosts beyond several state-of-the-art LP methods. Moreover, our LSH experiments demonstrate large speed gains without sacrificing accuracy. Our code and data is available at <https://github.com/abir-de/permgnn>.

1.3 Summary of contributions

(1) **Adversarial permutation guided embeddings:** We propose PERMGNN, a novel node embedding method, which provides high quality node representations for LP. In a sharp contrast to additive information aggregation in GNNs, we start with a permutation-sensitive but highly expressive aggregator of the graph neighbors and then desensitize the permutation-sensitivity by optimizing a min-max ranking loss function with respect to the smooth surrogates of adversarial permutations.

(2) **Hashing method for scalable predictions:** We propose an optimized binary transformation to the learnt node representations, that readily admits the use of a locality-sensitive hashing method and shows fast and accurate predictions.

(3) **Comprehensive evaluation:** We provide a rigorous evaluation to test both the representational power of PERMGNN and the proposed hashing method, which show that our proposal outperforms the respective state-of-the-art methods by a significant margin. Further probing the experimental results reveal insightful explanations behind the success of our methods.

2 Preliminaries

In this section, we describe necessary notations and the components of a typical LP system.

2.1 Notation

We consider a snapshot of an undirected social network $G = (V, E)$. Each node u has a feature vector f_u . We use $\text{nbr}(u)$ and $\overline{\text{nbr}}(u)$ to indicate the set of neighbors and non-neighbors of u . Our graphs do not have self edges, but we include u in $\text{nbr}(u)$ by convention. We define $\text{nbr}(u) = \{u\} \cup \{v \mid (u, v) \in E\}$, $\overline{\text{nbr}}(u) = \{v \mid v \neq u, (u, v) \notin E\}$ and also \overline{E} to be the set of non-edges, *i.e.*, $\overline{E} = \cup_{u \in V} \overline{\text{nbr}}(u)$. Finally, we define Π_δ to be the set of permutations of the set $[\delta] = \{1, 2, \dots, \delta\}$ and \mathcal{P}_δ to be the set of all possible 0/1 permutation matrices of size $\delta \times \delta$.

2.2 Scoring and ranking

Given a graph snapshot $G = (V, E)$, the goal of a LP algorithm is to identify node-pairs from the current set of non-edges \bar{E} (often called potential edges) that are likely to become edges in future. In principle, LP may be regarded as a classification task. An LP algorithm associates a latent binary variable with each potential edge and learns to predict it, after observing the current snapshot of the graph. In practice, most LP algorithms compute a **score** $s(u, v)$ for each potential edge $(u, v) \in \bar{E}$, which measures their likelihood of becoming connected in future. Recently invented network embedding methods [12, 17, 34] first learn a latent representation \mathbf{x}_u of each node $u \in V$ and then compute scores $s(u, v)$ using some similarity or distance measure between the corresponding representations \mathbf{x}_u and \mathbf{x}_v . In the test fold, some nodes are designated as *query* nodes q . Its (current) non-neighbors v are sorted by decreasing $s(q, v)$.

3 Proposed approach

In this section, we first state the limitations of GNNs and then describe our proposal for obtaining high quality node embeddings for LP, with better representational power than GNNs.

3.1 GNNs and their limitations

GNNs start with a graph and per-node features \mathbf{f}_u to obtain a neighborhood-sensitive node representation \mathbf{x}_u for $u \in V$. To meaningfully compare \mathbf{x}_u and \mathbf{x}_v and compute $s(u, v)$, information from neighbors of u (and v) should be aggregated in such a way that the embeddings become invariant to permutations of the neighbors of u (and v). GNNs ensure permutation invariance by additive aggregation. Given an integer K , for each node u , a GNN aggregates structural information k hops away from u to cast it into \mathbf{x}_u for $k \leq K$. Formally, a GNN first computes intermediate embeddings $\{\mathbf{z}_u(k) \mid k \in [K]\}$ in an iterative manner and then computes \mathbf{x}_u , using the following recurrent propagation rule.

$$\bar{\mathbf{z}}_u(k-1) = \text{AGGR}(\{\mathbf{z}_v(k-1) \mid v \in \text{nbr}(u)\}); \quad (1)$$

$$\mathbf{z}_u(k) = \text{COMB}_1(\mathbf{z}_u(k-1), \bar{\mathbf{z}}_u(k-1)); \quad (2)$$

$$\mathbf{x}_u = \text{COMB}_2(\mathbf{z}_u(1), \dots, \mathbf{z}_u(K)) \quad (3)$$

Here, for each node u with feature vector \mathbf{f}_u , we initialize $\mathbf{z}_u(0) = \mathbf{f}_u$; AGGR and $\text{COMB}_{1,2}$ are neural networks. To ensure permutation invariance of the final embedding \mathbf{x}_u , AGGR aggregates the intermediate $(k-1)$ -hop information $\mathbf{z}_v(k-1)$ with an additive (commutative, associative) function, guided by set function principles [52]:

$$\text{AGGR}(\{\mathbf{z}_v(k-1) \mid v \in \text{nbr}(u)\}) = \sigma_1 \left(\sum_{v \in \text{nbr}(u)} \sigma_2(\mathbf{z}_v(k-1)) \right). \quad (4)$$

Here σ_1, σ_2 are nonlinear activations. In theory [52, Theorem 2], if $\text{COMB}_{1,2}$ are given ‘sufficient’ hidden units, this set representation is universal. In practice, however, commutative-associative aggregation suffers from limited expressiveness [9, 30, 44], which degrades the quality of \mathbf{x}_u and $s(\cdot, \cdot)$, as described below. Specifically, their expressiveness is constrained from two perspectives.

Attenuation of important network signals. GNNs are established to be intrinsically low pass filters [29, 47]. Consequently, they can attenuate high frequency signals which may contain crucial structural information about the network. To illustrate, assume that the node u in Eqs. (1)–(3) has two neighbors v and w and $\mathbf{z}_v(k-1) = [+1, -1]$ and $\mathbf{z}_w(k-1) = [-1, +1]$, which induce high frequency signals around the neighborhood of u . In practice, these two representations may carry important signals about the network structure. However, popular choices of σ_2 often diminish the effect of each of these vectors. In fact, the widely used linear form of σ_2 [13, 17] would completely annul their effects (since $\sigma_2(\mathbf{z}_v(k-1)) + \sigma_2(\mathbf{z}_w(k-1)) = \mathbf{0}$) in the final embedding \mathbf{x}_u , which would consequently lose capacity for encapsulating neighborhood information.

Inability to distinguish between correlation structures. In Eq. (4), the outer nonlinearity σ_1 operates over the sum of all representations of neighbors of u . Therefore, it cannot explicitly model the variations between the joint dependence of these neighbors. Suppose the correlation between $\mathbf{z}_v(k-1)$ and $\mathbf{z}_w(k-1)$ is different from that between $\mathbf{z}_{v'}(k-1)$ and $\mathbf{z}_{w'}(k-1)$ for $\{v, v', w, w'\} \subseteq \text{nbr}(u)$. The additive aggregator in Eq. (4) cannot capture the distinction.

Here, we develop a mitigation approach which exploits sequential memory, e.g., LSTMs, even though they are order-sensitive, and then neutralize the order sensitivity by presenting adversarial neighbor orders. An alternative mitigation approach is to increase the capacity of the aggregator (while keeping it order invariant by design) by explicitly modeling

dependencies between neighbors, as has been attempted in image or text applications [5, 20, 38, 40, 41]. Appendix D compares these two approaches.

3.2 Our model: PERMGNN

Responding to the above limitations of popular GNN models, we design PERMGNN, the proposed adversarial permutation guided node embeddings.

3.2.1 Overview

Given a node u , we first compute an embedding \mathbf{x}_u using a *sequence* encoder, parameterized by θ :

$$\mathbf{x}_u = \rho_\theta(\{\mathbf{f}_v \mid v \in \text{nbr}(u)\}), \quad (5)$$

where $\text{nbr}(u)$ is presented in some arbitrary order (to be discussed). In contrast to the additive aggregator, ρ is modeled by an LSTM [14], followed by a fully-connected feedforward neural network (See Figure 1). Such a formulation captures the presence of high frequency signal in the neighborhood of u and the complex dependencies between the neighbors $\text{nbr}(u)$ by combining their influence via the recurrent states of the LSTM.

However, now the embedding \mathbf{x}_u is no longer invariant to the permutation of the neighbors $\text{nbr}(u)$. As we shall see, we counter this by casting the LP objective as an instance of min-max optimization problem. Such an adversarial setup refines \mathbf{x}_u in an iterative manner, to ensure that the resulting trained embeddings are permutation invariant (at least as far as possible in a non-convex optimization setting).

3.2.2 PERMGNN architecture

Let us suppose $\pi = [\pi_1, \dots, \pi_{|\text{nbr}(u)|}] \in \Pi_{|\text{nbr}(u)|}$ is some arbitrary permutation of the neighbors of node u . We take the features of neighbors of u in the order specified by π , i.e., $(v_{\pi_1}, v_{\pi_2}, \dots, v_{\pi_{|\text{nbr}(u)|}})$, and pass them into an LSTM:

$$\mathbf{y}_{u,1}, \dots, \mathbf{y}_{u,|\text{nbr}(u)|} = \text{LSTM}_\theta \left(\mathbf{f}_{v_{\pi_1}}, \dots, \mathbf{f}_{v_{\pi_{|\text{nbr}(u)|}}} \right). \quad (6)$$

Here $(\mathbf{y}_{u,k})_{k \in [|\text{nbr}(u)|]}$ is a sequence of intermediate representation of node u , which depends on the permutation π . Such an approach ameliorates the limitations of GNNs in two ways:

- Unlike GNNs, the construction of \mathbf{y}_\bullet is not limited to symmetric aggregation, and is therefore able to capture crucial network signals including those with high frequency [6].
- An LSTM (indeed, any RNN variant) is designed to capture the influence of one token of the sequence on the subsequent tokens. In the current context, the state variable \mathbf{h}_k of the LSTM combines the influence of first $k-1$ neighbors in the input sequence, i.e., $v_{\pi_1}, \dots, v_{\pi_{k-1}}$ on the k -th neighbor v_{π_k} . Therefore, these recurrent states allow \mathbf{y}_\bullet to capture the complex dependence between the features \mathbf{f}_\bullet .

Next, we compute the final embeddings \mathbf{x}_u by using an additional nonlinearity on the top of the sequence $(\mathbf{y}_{u,k})_{k \in [|\text{nbr}(u)|]}$ output by the LSTM:

$$\mathbf{x}_{u;\pi} = \sigma_\theta(\mathbf{y}_{u,1}, \mathbf{y}_{u,2}, \dots, \mathbf{y}_{u,|\text{nbr}(u)|}) \in \mathbb{R}^D. \quad (7)$$

Note that the embeddings $\{\mathbf{x}_u\}$ computed above depends on π , the permutation of the neighbors $\text{nbr}(u)$ given as the input sequence to the LSTM in Eq. (6).

Removing the sensitivity to π . One simple way to ensure permutation invariance is to compute the average of $\mathbf{x}_{u;\pi}$ over all possible permutations $\pi \in \Pi_{|\text{nbr}(u)|}$. At a time and space complexity of at least $O(\sum_{u \in V} |\Pi_{|\text{nbr}(u)|}|)$, this is quite impractical for even moderate degree nodes. Replacing the exhaustive average by a Monte Carlo sample does improve representation quality, but is still very expensive. Murphy et al. [28] proposed a method called π -SGD, which samples one permutation per epoch. While it is more efficient than sampling multiple permutations, it shows worse robustness in practice.

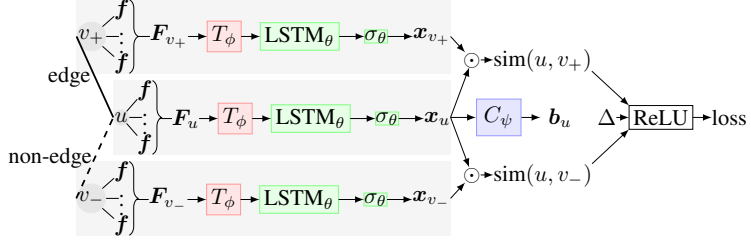


Figure 1: PERMGNN min-max loss and hashing schematic. Given a node u , we first pass all the features of its neighbors v_+ (and non-neighbors v_-) through the Sinkhorn permutation operator T_ϕ , which outputs a permuted sequence of features. This permuted sequence of features is fed into an LSTM with parameters θ , whose output is given as input to the final layer σ_θ to compute the embedding x_u . These node embeddings are finally used to compute the similarity scores of u with the neighbors and non-neighbors. These similarity scores are fed into the pairwise ranking loss function for training θ and ϕ . Additionally we also train a network C_ψ , which converts x_u into hashcodes b_u .

3.2.3 Adversarial permutation-driven LP objective

Instead of brute-force sampling, we setup a two-party game, one being the network for LP, vulnerable to π , and the other being an adversary, which tries to make the LP network perform poorly by choosing a ‘bad’ π at each node.

- 1: pick initial π^u at each node u
- 2: **repeat**
- 3: fix $\{\pi^u : u \in V\}$; optimize θ for best LP accuracy
- 4: fix θ ; find next π^u at all u for worst LP accuracy
- 5: **until** LP performance stabilizes

Let $\pi^u \in \Pi_{|\text{nbr}(u)|}$ be the permutation used to shuffle the neighbors of u in Eq. (6). Conditioned on π^u, π^v , we compute the score for a node-pair (u, v) as

$$s_\theta(u, v | \pi^u, \pi^v) = \text{sim}(\mathbf{x}_{u; \pi^u}, \mathbf{x}_{v; \pi^v}), \quad (8)$$

where $\text{sim}(\mathbf{a}, \mathbf{b})$ denotes the cosine similarity between \mathbf{a} and \mathbf{b} . To train our LP model to give high quality ranking, we consider the following AUC loss surrogate [15]:

$$\text{loss}(\theta; \{\pi^w\}_{w \in V}) = \sum_{\substack{(u, v) \in E \\ (r, t) \in \overline{E}}} \left[\Delta + s_\theta(r, t | \pi^r, \pi^t) - s_\theta(u, v | \pi^u, \pi^v) \right]_+ \quad (9)$$

where Δ is a tunable margin and $[a]_+ = \max\{0, a\}$.

As stated above, we aim to train LP model parameters θ in such a way that the trained embeddings $\{\mathbf{x}_u\}$ become invariant to the permutations of $\text{nbr}(u)$ for all nodes $u \in V$. This requirement suggests the following min-max loss:

$$\min_{\theta} \max_{\{\pi^w\}_{w \in V}} \text{loss}(\theta; \{\pi^w\}_{w \in V}). \quad (10)$$

3.2.4 Neural permutation surrogate

As stated, the complexity of Eq. (10) seems no better than exhaustive enumeration of permutations. To get past this apparent blocker, just as max is approximated by softmax (a multinomial distribution), a ‘hard’ permutation (1:1 assignment) π^w is approximated by a ‘soft’ permutation matrix \mathbf{P}^w — a doubly stochastic matrix — which allows continuous optimization.

Suppose $\mathbf{F}_w = [\mathbf{f}_{v_1}, \mathbf{f}_{v_2}, \dots, \mathbf{f}_{v_{|\text{nbr}(w)|}}]$ is a matrix whose rows are formed by the features of $\text{nbr}(w)$ presented in some canonical order. Then $\mathbf{P}^w \mathbf{F}_w$ approximates a permuted feature matrix corresponding to some permuted sequence of neighbor feature vectors. The rhs of Eq. (6) can be written as $\text{LSTM}_\theta(\mathbf{P}^w \mathbf{F}_w)$, which eventually lets us express loss as a function of \mathbf{P}^w . We can thus rewrite the min-max optimization (10) as

$$\min_{\theta} \max_{\{\mathbf{P}^w | w \in V\}} \text{loss}(\theta; \{\mathbf{P}^w\}_{w \in V}), \quad (11)$$

where the inner maximization is carried out over all ‘soft’ permutation matrices \mathbf{P}^w , parameterized as follows.

In deep network design, a trainable multinomial distribution is readily obtained by applying a softmax to trainable (unconstrained) logits. Analogously, a trainable soft permutation matrix \mathbf{P}^w can be obtained by applying a Gumbel-Sinkhorn network ‘GS’ [26] to a trainable (unconstrained) ‘seed’ square matrix, say, \mathbf{A}^w :

$$\begin{aligned}\mathbf{P}^w &= \lim_{n \rightarrow \infty} \text{GS}^n(\mathbf{A}^w), \quad \text{where} \\ \text{GS}^0(\mathbf{A}^w) &= \exp(\mathbf{A}^w) \quad \text{and} \\ \text{GS}^n(\mathbf{A}^w) &= \text{COLSCALE}(\text{ROWSCALE}(\text{GS}^{n-1}(\mathbf{A}^w))).\end{aligned}$$

Here, **COLSCALE** and **ROWSCALE** represent column and row normalization. $\text{GS}^n(\mathbf{A}^w)$ is the doubly stochastic matrix obtained by consecutive row and column normalizations of \mathbf{A}^w . It can be shown that

$$\lim_{n \rightarrow \infty} \text{GS}^n(\mathbf{A}^w) = \underset{\mathbf{P} \in \mathcal{P}_{|\text{nbr}(w)|}}{\text{argmax}} \text{Tr}[\mathbf{P}^\top \mathbf{A}^w]. \quad (12)$$

GS^n thus represents a recursive differentiable operator that permits backpropagation of loss to $\{\mathbf{A}^w\}$. In practice, n is a finite hyperparameter, the larger it is, the closer the output to a ‘hard’ permutation.

Allocating a separate unconstrained seed matrix \mathbf{A}^w for each node w would lead to an impractically large number of parameters. Therefore, we express \mathbf{A}^w using a globally shared network \mathbf{T}_ϕ with model weights ϕ , and the per-node feature matrix \mathbf{F}_w already available. I.e., we define

$$\mathbf{A}^w := \mathbf{T}_\phi(\mathbf{F}_w / \tau), \quad (13)$$

where $\tau > 0$ is a temperature hyperparameter that encourages $\text{GS}^n(\mathbf{A}^w)$ toward a ‘harder’ soft permutation. The above steps allow us to rewrite optimization (11) in terms of θ and ϕ in the form $\min_\theta \max_\phi \text{loss}(\theta; \phi)$. After completing the min-max optimization, the embedding \mathbf{x}_u of a node u can be computed using some arbitrary neighbor permutation. By design, the impact on $\text{sim}(u, v)$ is small when different permutations are used. Appendix C contains further implementation details.

4 Scalable LP by hashing representations

At this point, we have obtained representations \mathbf{x}_u for each node u using PERMGNN. Our next goal is to infer some number of most likely future edges.

Prediction using exhaustive comparisons. Here, we first enumerate the scores for all possible potential edges (the current non-edges) and then report top- K neighbors for each node. Since most real-life social networks are sparse, potential edges can be $\Theta(|V|^2)$ in number. Scoring all of them in large graphs is impractical; we must limit the number of comparisons between potentially connecting node pairs to be as small as possible. To that aim, we first present the well known random hyperplane based hashing method and then present our proposed method.

4.1 Data-oblivious LSH with random hyperplanes

When for two nodes u and v , $\text{sim}(u, v)$ is defined as $\cos(\mathbf{x}_u, \mathbf{x}_v)$ with $\mathbf{x}_\bullet \in \mathbb{R}^D$, the classic random hyperplane LSH can be used to hash the embeddings \mathbf{x}_\bullet . Specifically, we first draw H uniformly random hyperplanes passing through the origin in the form of their unit normal vectors $\mathbf{n}_h \in \mathbb{R}^D, h \in [H]$ [7]. Then we set $b_u[h] = \text{sign}(\mathbf{n}_h \cdot \mathbf{x}_u) \in \pm 1$ as a 1-bit hash and $\mathbf{b}_u \in \pm 1^H$ as the H -bit hash code of node u . Correspondingly, we set up 2^H hash buckets with each node going into one bucket. If the buckets are balanced, we expect each to have $N/2^H$ nodes. Now we limit pairwise comparisons to only node pairs within each bucket, which takes $N^2/2^H$ pair comparisons. By letting H grow slowly with N , we can thus achieve sub-quadratic time. However, such a hashing method is data oblivious—the hash codes are not learned from the distribution of the original embeddings \mathbf{x}_\bullet . In fact, it shows good performance only when the embeddings are uniformly dispersed in the D -dimensional space, so that the random hyperplanes can evenly distribute the nodes within the several hash buckets.

```

1: Input: Graph  $G = (V, E)$ ; binary hash-codes  $\{\mathbf{b}_u\}$ ; query nodes  $Q$ ; the number ( $K$ ) of nodes to be recommended per query node
2: Output: Ranked recommendation list  $R_q$  for all  $q \in Q$ 
3: initialize LSH buckets
4: for  $u \in V$  do
5:   add  $u$  to appropriate hash buckets
6: for  $q \in Q$  do
7:   initialize score heap  $H_q$  with capacity  $K$ 
8: for each LSH bucket  $B$  do
9:   for  $(u, v) \in B$  do
10:    if  $u \in Q$  then
11:      insert  $\langle v, s(u, v) \rangle$  in  $H_u$ ; prune if  $|H_u| > K$ 
12:    if  $v \in Q$  then
13:      insert  $\langle u, s(u, v) \rangle$  in  $H_v$ ; prune if  $|H_v| > K$ 
14: for  $q \in Q$  do
15:   sort  $H_q$  by decreasing score to get ranked list  $R_q$ 
16: return  $\{R_q | q \in Q\}$ 

```

Algorithm 1: Reporting ranked list of potential edges fast.

4.2 Learning data-sensitive hash codes

To overcome the above limitation of random hyperplane based hashing, we devise a data-driven learning of hash codes as explored in other applications [46]. Specifically, we aim to design an additional transformation of the vectors $\{\mathbf{x}_u\}$ into compressed representations $\{\mathbf{b}_u\}$, with the aim of better balance across hash buckets and reduced prediction time.

4.2.1 Hashing/compression network

In what follows, we will call the compression network $C_\psi : \mathbb{R}^D \rightarrow [-1, 1]^H$, with model parameters ψ . We interpret $\text{sign}(C_\psi(\mathbf{x}_u))$ as the required binary hash code $\mathbf{b}_u \in \{-1, +1\}^H$, with the surrogate $\tanh(C_\psi(\mathbf{x}_u))$, to be used in the following smooth optimization:

$$\begin{aligned} \min_{\psi} & \frac{\alpha}{|V|} \sum_{u \in V} |\mathbf{1}^\top \tanh(C_\psi(\mathbf{x}_u))| + \frac{\beta}{|V|} \sum_{u \in V} \left\| |\tanh(C_\psi(\mathbf{x}_u))| - \mathbf{1} \right\|_1 \\ & + \frac{\gamma}{|\overline{E}|} \sum_{(u, v) \in \overline{E}} |\tanh(C_\psi(\mathbf{x}_u)) \cdot \tanh(C_\psi(\mathbf{x}_v))| \end{aligned} \quad (14)$$

Here, \overline{E} is the set of non-edges and $\alpha, \beta, \gamma \in (0, 1)$, with $\alpha + \beta + \gamma = 1$ are tuned hyperparameters. The final binary hash code $\mathbf{b}_u = \text{sign}(C_\psi(\mathbf{x}_u))$. The salient terms in the objective above seek the following goals.

Bit balance: If each bit position has as many -1 s as $+1$ s, that bit evenly splits the nodes. The term $|\mathbf{1}^\top \tanh(C_\psi(\mathbf{x}_u))|$ tries to bit-balance the hash codes.

No sitting on the fence: The optimizer is prevented from setting $\mathbf{b} = \mathbf{0}$ (the easiest way to balance it) by including a term $\sum_h \|\mathbf{b}[h] - 1\| = \|\mathbf{b} - \mathbf{1}\|_1$.

Weak supervision: The third term encourages currently unconnected nodes to be assigned dissimilar bit vectors.

4.2.2 Bucketing and ranking

Note that, we do not expect the dot product between the learned hash codes $\mathbf{b}_u \cdot \mathbf{b}_v$ to be a good approximation for $\cos(\mathbf{x}_u, \mathbf{x}_v)$, merely that node pairs with large $\cos(\mathbf{x}_u, \mathbf{x}_v)$ will be found in the same hash buckets. We form the buckets using the recipe of Gionis et al. [11] (details in Appendix B). We adopt the high-recall policy that node-pair u, v should be scored if u and v share at least one bucket. Algorithm 1 shows how the buckets are traversed to generate and score node pairs, then placed in a heap for retrieving top- K pairs.

	Mean Average Precision (MAP)					Mean Reciprocal Rank (MRR)				
	Twitter	Google+	Cora	Citeseer	PB	Twitter	Google+	Cora	Citeseer	PB
AA	0.644	0.263	0.318	0.400	0.164	0.839	0.508	0.412	0.455	0.423
CN	0.614	0.234	0.284	0.367	0.134	0.824	0.495	0.369	0.405	0.407
Node2Vec	0.621	0.272	0.369	0.464	0.135	0.838	0.472	0.422	0.515	0.255
DeepWalk	0.581	0.227	0.356	0.449	0.136	0.776	0.403	0.402	0.491	0.248
GraphSAGE	0.668	0.244	0.291	0.380	0.109	0.782	0.357	0.307	0.386	0.188
GCN	0.630	0.287	0.353	0.455	0.142	0.812	0.433	0.397	0.497	0.268
SEAL	0.652	0.376	0.382	0.420	0.302	0.837	0.661	0.486	0.483	0.630
Gravity	0.686	0.326	0.351	0.447	0.158	0.839	0.490	0.398	0.497	0.286
PERMGNN	0.910	0.630	0.923	0.936	0.425	0.972	0.752	0.939	0.941	0.609

Table 1: MAP and MRR for all LP algorithms (PERMGNN and eight baselines) on the ranked list of all potential edges ($K = \infty$) across all five datasets, with 40% test set. Numbers in bold font (boxes) indicate the best performer (resp. second best performer). PERMGNN outperforms all baselines in almost all scenarios except for MRR in PB.

5 Experiments

We report on a comprehensive evaluation of PERMGNN and its accompanying hashing strategy. Specifically, we address the following research questions. **RQ1:** Does PERMGNN lead to LP accuracy better than state-of-the-art link predictors? Where are the gains and losses? **RQ2:** How does PERMGNN compare with brute-force sampling of neighbor permutations? **RQ3:** Exactly where in our adversarially trained network is permutation insensitivity getting programmed? **RQ4:** Does the hashing optimization reduce prediction time, compared to exhaustive computation of pairwise scores? (Appendix D describes additional experiments.)

5.1 Experimental setup

5.1.1 Datasets

We consider five real world datasets summarized in Appendix C: (1) Twitter [21], (2) Google+ [22], (3) Cora [10, 37], (4) Citeseer [10, 37] and (5) PB [1].

5.1.2 Baselines

We compare PERMGNN with eight state-of-the-art LP algorithms. More specifically, we consider two unsupervised approaches that only exploit local signals to compute the LP scores: (1) Adamic Adar (AA) and (2) Common Neighbors (CN) [23]; two embedding models based on random walks on graph: (3) Node2Vec [12] and (4) DeepWalk [31]; also four embedding models based on GNNs: (5) GraphSAGE [13], (6) Graph Convolutional Network (GCN) [18], (7) SEAL [53] and (8) Gravity [34]. For PERMGNN and deep embeddings, we set $D = \dim(\mathbf{x}_\bullet)$ and $H = \dim(C_\psi(\mathbf{x}_\bullet))$ as 16.

In Appendix D, we also evaluate the alternative of richer transformer-based set aggregators [20] that are order invariant by design.

5.1.3 Evaluation protocol

Similar to several state-of-the-art LP models [12, 18, 23], we partition the edge (and non-edge) sets into training, validation and test folds as follows. For each dataset, we first build the set of query nodes Q , where each query contains at least one triangle around it. Then for each $q \in Q$, in the original graph, we partition the neighbors $\text{nbr}(q)$ and the non-neighbors $\overline{\text{nbr}}(q)$ into 54% training, 6% validation and 40% test sets, where the corresponding node pairs are sampled uniformly at random. We disclose the resulting sampled graph induced by the training and validation sets to the LP model. Then, for each query $q \in Q$, the trained LP model outputs a top- K list of potential neighbors from the test set. From ground truth, we compute the average precision (AP) and reciprocal rank (RR) of each top- K list. Then we average over all query nodes to get mean AP (MAP) and mean RR (MRR). Further details of evaluation can be found in Appendix C.

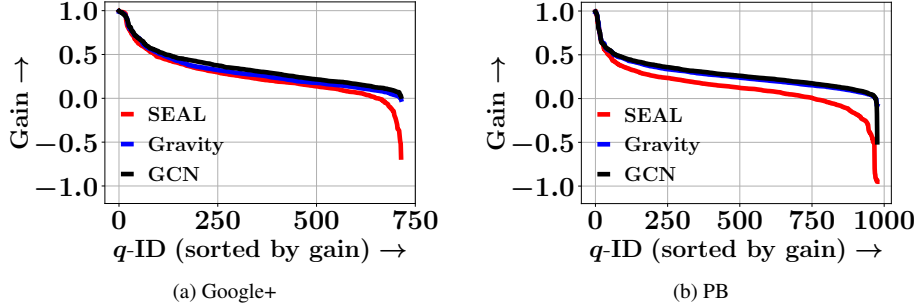


Figure 2: Improvement of performance in terms of $AP(\text{PERMGNN}) - AP(\text{baseline})$, the gain (above x-axis) or loss (below x-axis) of AP of PERMGNN with respect to three competitive baselines: SEAL, GCN and Gravity across different queries for Google+ and PB datasets. Queries Q sorted by decreasing gain of PERMGNN along x -axis.

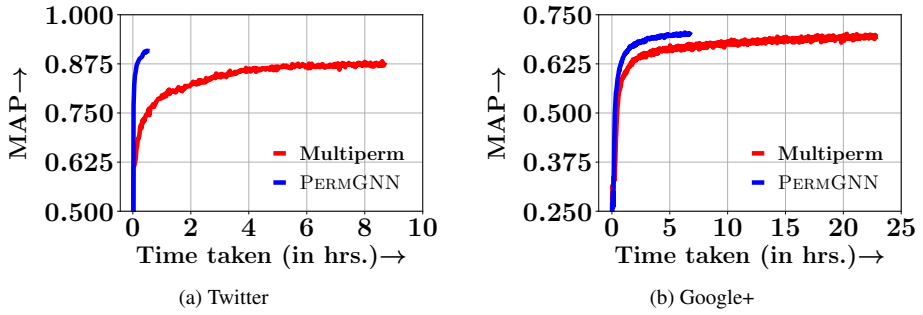


Figure 3: Validation MAP against training epochs for Twitter and Google+. PERMGNN converges faster than MultiPerm.

5.2 Comparative analysis of LP accuracy

First, we address the research question **RQ1** by comparing LP accuracy of PERMGNN against baselines, in terms of MAP and MRR across all the datasets. Here, we enumerated the pairwise scores using exhaustive comparisons.

5.2.1 MAP and MRR summary

Table 1 summarizes LP accuracy across all the methods. We make the following observations. (1) PERMGNN outperforms all the competitors by a substantial margin, in almost all the scenarios, except PB, where it is outperformed by SEAL in terms of MRR. Furthermore, whenever PERMGNN outperforms baselines, it shows significantly better performance (both MAP and MRR) than the nearest baseline at p-values less than 0.001. (2) The performance of GNNs are comparable. In particular, SEAL is the second best performer in Google+, Cora and PB datasets. It learns to extract the key subgraph explaining the presence or absence of a link. Such an approach allows it to outperform the alternative GNN based methods. (3) The unsupervised predictors, *i.e.*, AA and CN often beat some of embedding models. Together with Gravity, AA is the second best performer in terms of MRR in Twitter. Since AA and CN encourage triad completion, which is a key factor for growth of several real life networks, they often serve as good link predictors [35]. (4) The random walk based embeddings, *viz.* Node2Vec and DeepWalk, show moderate performance. Notably, Node2Vec is the second best performer in Citeseer.

5.2.2 Drill-down

Next we compare ranking performance at individual query nodes. For each query (node) q , we measure the gain (or loss) of PERMGNN in terms of average precision, *i.e.*, $AP(\text{PERMGNN}) - AP(\text{baseline})$ for three competitive baselines, across Google+ and PB datasets. From Figure 2 we observe that (1) PERMGNN outperforms the baselines for more than 91% and 75% of all the queries, across Google+ and PB datasets respectively; (2) for more than 43% queries in Google+, PERMGNN gains at least 0.25 MAP against the nearest competitor.

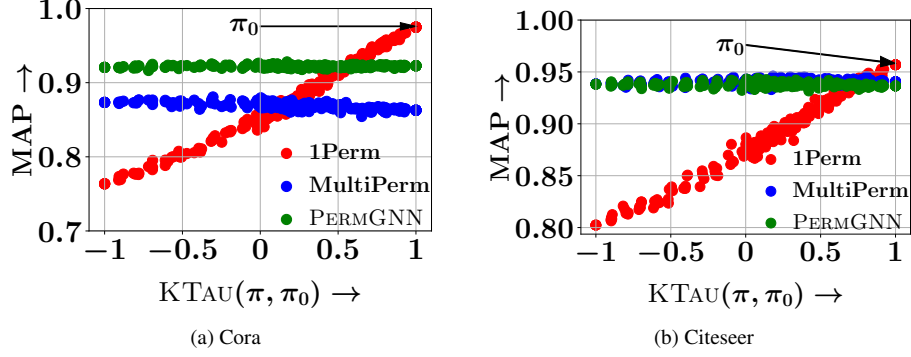


Figure 4: Effect of neighbor order perturbation on MAP. As we move away from the canonical permutation π_0 , MAP values deteriorate for 1Perm, but it remains roughly same for both MultiPerm and PERMGNN.

5.3 PERMGNN vs. sampling permutations

Next, we address research question **RQ2** by establishing the utility of PERMGNN against its natural alternative **MultiPerm**, in which a node embedding is computed by averaging permutation-sensitive representations over several sampled permutations. Figure 3 shows that PERMGNN is $\sim 17\times$ faster and $\sim 3\times$ faster than the permutation averaging based method for Twitter and Google+ datasets. MultiPerm also occupies significantly larger RAM than PERMGNN.

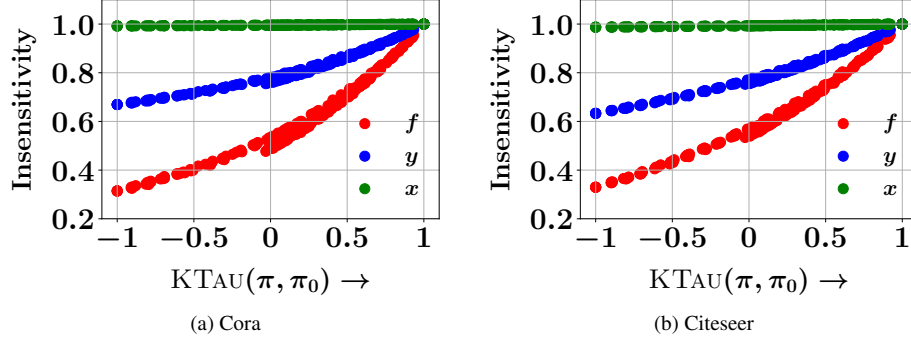


Figure 5: Insensitivity of neighborhood features $\{f_v \mid v \in \text{nbr}(u)\}$ LSTM output $\{y\}$ and the resultant node embeddings x_u with respect to neighbor order permutations.

5.4 Permutation invariance of PERMGNN

Here, we answer the research question **RQ3**. To that end, we first train PERMGNN along with its two immediate alternatives: (i) **1Perm** where a vanilla LSTM is trained with a single canonical permutation π_0 of the nodes; and, (ii) **MultiPerm** where an LSTM is trained using several permutations of the nodes. Then, given a test permutation π , we compute the node embedding $x_{u;\pi}$ by feeding the corresponding sequence of neighbors $\pi(\text{nbr}(u))$ (sorted by node IDs of $\text{nbr}(u)$ assigned by π), as an input to the trained models. Finally, we use these embeddings for LP and investigate the effect of the π on the MAP value. Figure 4 captures this effect by showing the variation of $\text{MAP}(\pi)$ against the correlation between π and the canonical order π_0 , measured in terms of Kendall’s τ — $\text{KTAU}(\pi, \pi_0)$, for Cora and Citeseer datasets. It reveals that, 1Perm suffers a significant drop in LP accuracy when the input node order π substantially differs from the canonical order π_0 , *i.e.*, $\text{KTAU}(\pi, \pi_0)$ is low. However, both MultiPerm and PERMGNN turns out to be permutation-insensitive across a wide range of node orderings, thanks to the underlying design.

But what is the secret behind the impressive resilience of PERMGNN? Is it because the input feature sequence $\{f_v\}$ was already permutation invariant, or has the model learned to be so, assisted by adversarial training? To answer this question, we further instrument the stability of f, y, x to different permutations. Specifically, we probe the variation of insensitivity of the input sequence $\{f_v : v \in \text{nbr}(u)\}$, the intermediate LSTM output $\{y\}$ and the final embedding x_u

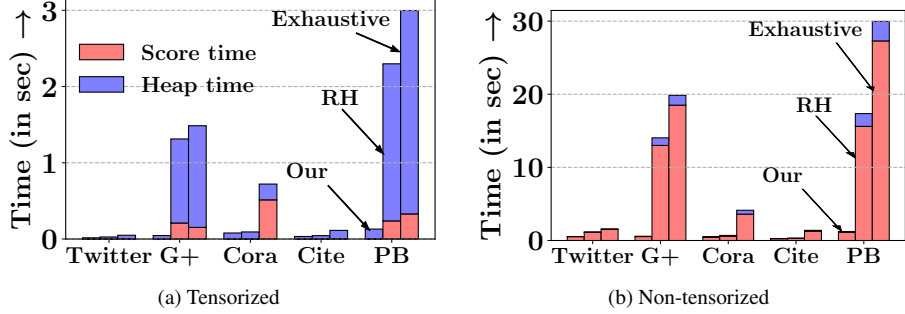


Figure 6: Running time for our LSH based scalable prediction, random-hyperplane based LSH method, exhaustive comparison. Our scalable prediction offers significant time savings against exhaustive enumeration.

	Twitter	Google+	Cora	Citeseer	PB
Hashing on $C_\psi(\mathbf{x})$	+1.92%	+8.46%	+3.43%	+0.73%	+8.32%
Random hyperplanes	+0.37%	+0.42%	+2.97%	-0.45%	-2.35%

Table 2: Hashing increases MAP by a few percent.

with respect to different permutations π , where $\text{insensitivity}(\mathbf{z}; \pi, \pi_0) = \sum_{u \in V} \text{SIM}(\mathbf{z}_{u; \pi}, \mathbf{z}_{u; \pi_0})/|V|$ for any vector or sequence \mathbf{z} . Figure 5 summarizes the results, which show that as the computation within the model progresses, from input feature sequence to the final embeddings, the insensitivity of the underlying signals increases. Such an observation indicates that our adversarial training smoothly turns permutation-sensitive input sequences into permutation invariant node embeddings, without using any explicit symmetric aggregator.

5.5 Performance of hashing methods

Next, we study the performance of our LSH method (Section 4.2), which addresses the research question **RQ4**. Specifically, we compare the time spent in similarity computation and heap operations of our hashing method against random hyperplane based hashing (Section 4.1) and exhaustive computation of pairwise scores. Since vectorized similarity computation inside Torch may be faster than numpy, we provide results on both implementations. Figure 6 summarizes the results, which shows that: (1) hashing using C_ψ leads to considerable savings in reporting top- K node-pairs with respect to both random hyperplane based hashing and exhaustive enumeration, (2) the gains increase with increasing graph sizes (from Google+ to PB). Moreover, from Table 2, we notice a small improvement in MAP values, instead of the expected minor degradation. This is entirely possible given the highly non-convex optimizations involved.

6 Conclusion

We presented PERMGNN, a novel LP formulation that combines a recurrent, order-sensitive graph neighbor aggregator with an adversarial generator of neighbor permutations. PERMGNN achieves LP accuracy comparable with or better than sampling a number of permutations by brute force, and is much faster. PERMGNN is also superior to a number of recent and ancient LP baselines. In addition, we formulate an optimization to map PERMGNN’s node embeddings to a suitable locality-sensitive hash, which greatly speeds up reporting of the most likely edges. It would be interesting to extend PERMGNN to other downstream applications for networks, *e.g.*, node classification, community detection, knowledge graph completion, etc.

References

- [1] R. Ackland et al. Mapping the us political blogosphere: Are conservative bloggers more prominent? In *BlogTalk Downunder 2005 Conference, Sydney*. BlogTalk Downunder 2005 Conference, Sydney, 2005.
- [2] L. A. Adamic and E. Adar. Friends and neighbors on the Web. *Social Networks*, 25(3):211 – 230, 2003. ISSN 0378-8733. doi: [http://dx.doi.org/10.1016/S0378-8733\(03\)00009-1](http://dx.doi.org/10.1016/S0378-8733(03)00009-1). URL <http://pkudlib.org/qmeiCourse/files/FriendsAndNeighbors.pdf>.

- [3] L. Backstrom and J. Leskovec. Supervised random walks: predicting and recommending links in social networks. In *WSDM Conference*, pages 635–644, 2011. URL <http://cs.stanford.edu/people/jure/pubs/linkpred-wsdm11.pdf>.
- [4] A.-L. Barabási and R. Albert. Emergence of scaling in random networks. *science*, 286(5439):509–512, 1999.
- [5] B. Bloem-Reddy and Y. W. Teh. Probabilistic symmetry and invariant neural networks. *arXiv preprint arXiv:1901.06082*, 2019.
- [6] S. Borovkova and I. Tsiamas. An ensemble of lstm neural networks for high-frequency stock market classification. *Journal of Forecasting*, 38(6):600–619, 2019.
- [7] M. S. Charikar. Similarity estimation techniques from rounding algorithms. In *STOC*, pages 380–388, 2002. URL <https://dl.acm.org/doi/pdf/10.1145/509907.509965>.
- [8] M. Cuturi. Sinkhorn distances: Lightspeed computation of optimal transport. In *NeurIPS*, pages 2292–2300, 2013. URL <https://papers.nips.cc/paper/4927-sinkhorn-distances-lightspeed-computation-of-optimal-transport.pdf>.
- [9] V. K. Garg, S. Jegelka, and T. Jaakkola. Generalization and representational limits of graph neural networks. *arXiv preprint arXiv:2002.06157*, 2020.
- [10] L. Getoor. Link-based classification. In *Advanced methods for knowledge discovery from complex data*, pages 189–207. Springer, 2005.
- [11] A. Gionis, P. Indyk, and R. Motwani. Similarity search in high dimensions via hashing. In *VLDB Conference*, pages 518–529, 1999. See <http://citesear.nj.nec.com/gionis97similarity.html>.
- [12] A. Grover and J. Leskovec. node2vec: Scalable feature learning for networks. In *SIGKDD*, 2016.
- [13] W. Hamilton, Z. Ying, and J. Leskovec. Inductive representation learning on large graphs. In *Advances in neural information processing systems*, pages 1024–1034, 2017.
- [14] S. Hochreiter and J. Schmidhuber. Long short-term memory. *Neural Computation*, 9(8):1735–1780, 1997. URL <https://www.mitpressjournals.org/doi/pdfplus/10.1162/neco.1997.9.8.1735>.
- [15] T. Joachims. A support vector method for multivariate performance measures. In *ICML*, pages 377–384, 2005. ISBN 1-59593-180-5. doi: <http://doi.acm.org/10.1145/1102351.1102399>. URL http://www.machinelearning.org/proceedings/icml2005/papers/048_ASupport_Joachims.pdf.
- [16] B. Katz. From sentence processing to information access on the World wide Web. In *AAAI Spring Symposium on Natural Language Processing for the World Wide Web*, pages 77–94, Stanford CA, 1997. Stanford University. See <http://www.ai.mit.edu/people/boris/webaccess/>.
- [17] T. N. Kipf and M. Welling. Semi-supervised classification with graph convolutional networks. *arXiv preprint arXiv:1609.02907*, 2016.
- [18] T. N. Kipf and M. Welling. Variational graph auto-encoders. *arXiv preprint arXiv:1611.07308*, 2016.
- [19] B. Kulis and T. Darrell. Learning to hash with binary reconstructive embeddings. In *NeurIPS*, pages 1042–1050, 2009. URL <https://papers.nips.cc/paper/3667-learning-to-hash-with-binary-reconstructive-embeddings.pdf>.
- [20] J. Lee, Y. Lee, J. Kim, A. Kosiorek, S. Choi, and Y. W. Teh. Set transformer: A framework for attention-based permutation-invariant neural networks. In *ICML*, 2019.
- [21] J. Leskovec and J. J. Mcauley. Learning to discover social circles in ego networks. In *NeurIPS*, 2012.
- [22] J. Leskovec, D. Chakrabarti, J. Kleinberg, C. Faloutsos, and Z. Ghahramani. Kronecker graphs: An approach to modeling networks. *Journal of Machine Learning Research*, 11(Feb):985–1042, 2010.
- [23] D. Liben-Nowell and J. Kleinberg. The link-prediction problem for social networks. *Journal of the American Society for Information Science and Technology*, 58(7):1019–1031, 2007. ISSN 1532-2890. doi: 10.1002/asi.20591. URL <https://onlinelibrary.wiley.com/doi/full/10.1002/asi.20591>.
- [24] R. N. Lichtenwalter, J. T. Lussier, and N. V. Chawla. New perspectives and methods in link prediction. In *SIGKDD Conference*, pages 243–252, Washington, DC, USA, 2010. ACM. ISBN 978-1-4503-0055-1. doi: 10.1145/1835804.1835837. URL http://users.cs.fiu.edu/~1zhen001/activities/KDD_USB_key_2010/docs/p243.pdf.
- [25] W. Liu, J. Wang, R. Ji, Y.-G. Jiang, and S.-F. Chang. Supervised hashing with kernels. In *IEEE CVPR*, pages 2074–2081, 2012. URL <https://ieeexplore.ieee.org/stamp/stamp.jsp?arnumber=6247912>.
- [26] G. Mena, D. Belanger, S. Linderman, and J. Snoek. Learning latent permutations with gumbel-sinkhorn networks. *arXiv preprint arXiv:1802.08665*, 2018. URL <https://arxiv.org/pdf/1802.08665.pdf>.
- [27] R. L. Murphy, B. Srinivasan, V. Rao, and B. Ribeiro. Janossy pooling: Learning deep permutation-invariant functions for variable-size inputs. *ICLR*, 2019. URL <https://arxiv.org/pdf/1811.01900.pdf>.
- [28] R. L. Murphy, B. Srinivasan, V. Rao, and B. Ribeiro. Relational pooling for graph representations. *arXiv preprint arXiv:1903.02541*, 2019.
- [29] H. NT and T. Maehara. Revisiting graph neural networks: All we have is low-pass filters. *arXiv preprint arXiv:1905.09550*, 2019.
- [30] C. Pabbaraju and P. Jain. Learning functions over sets via permutation adversarial networks. *arXiv preprint arXiv:1907.05638*, 2019. URL <https://arxiv.org/pdf/1907.05638.pdf>.

[31] B. Perozzi, R. Al-Rfou, and S. Skiena. Deepwalk: Online learning of social representations. In *KDD*, pages 701–710, 2014.

[32] C. R. Qi, H. Su, K. Mo, and L. J. Guibas. Pointnet: Deep learning on point sets for 3d classification and segmentation. In *Proceedings of the IEEE conference on computer vision and pattern recognition*, pages 652–660, 2017.

[33] S. Ravanbakhsh, J. Schneider, and B. Poczos. Deep learning with sets and point clouds. *arXiv preprint arXiv:1611.04500*, 2016.

[34] G. Salha, S. Limnios, R. Hennequin, V.-A. Tran, and M. Vazirgiannis. Gravity-inspired graph autoencoders for directed link prediction. In *CIKM*, page 589–598, 2019. URL <https://doi.org/10.1145/3357384.3358023>.

[35] P. Sarkar, D. Chakrabarti, and A. W. Moore. Theoretical justification of popular link prediction heuristics. In *COLT*, 2011.

[36] M. Schlichtkrull, T. N. Kipf, P. Bloem, R. Van Den Berg, I. Titov, and M. Welling. Modeling relational data with graph convolutional networks. In *European Semantic Web Conference*, pages 593–607, 2018. URL <https://arxiv.org/pdf/1703.06103.pdf>.

[37] P. Sen, G. Namata, M. Bilgic, L. Getoor, B. Galligher, and T. Eliassi-Rad. Collective classification in network data. *AI magazine*, 29(3):93–93, 2008.

[38] Y. Shi, J. Oliva, and M. Niethammer. Deep message passing on sets. In *AAAI*, pages 5750–5757, 2020.

[39] R. Sinkhorn. Diagonal equivalence to matrices with prescribed row and column sums. *The American Mathematical Monthly*, 74(4):402–405, 1967. URL <https://www.jstor.org/stable/pdf/2314570.pdf>.

[40] K. Skianis, G. Nikolentzos, S. Limnios, and M. Vazirgiannis. Rep the set: Neural networks for learning set representations. In *International Conference on Artificial Intelligence and Statistics*, pages 1410–1420. PMLR, 2020.

[41] K. Stelzner, K. Kersting, and A. R. Kosiorek. Generative adversarial set transformers. In *Workshop on Object-Oriented Learning at ICML 2020*, 2020. URL https://www.ml.informatik.tu-darmstadt.de/papers/stelzner2020ood_gast.pdf.

[42] J. Tang, M. Qu, M. Wang, M. Zhang, J. Yan, and Q. Mei. LINE: Large-scale information network embedding. In *WWW Conference*, pages 1067–1077, 2015.

[43] P. Veličković, G. Cucurull, A. Casanova, A. Romero, P. Lio, and Y. Bengio. Graph attention networks. *arXiv preprint arXiv:1710.10903*, 2017.

[44] E. Wagstaff, F. B. Fuchs, M. Engelcke, I. Posner, and M. Osborne. On the limitations of representing functions on sets. *arXiv preprint arXiv:1901.09006*, 2019.

[45] Z. Wang, Z. Ren, C. He, P. Zhang, and Y. Hu. Robust embedding with multi-level structures for link prediction. In *IJCAI*, pages 5240–5246, 2019. URL <https://www.ijcai.org/Proceedings/2019/0728.pdf>.

[46] Y. Weiss, A. Torralba, and R. Fergus. Spectral hashing. In *NeurIPS*, pages 1753–1760, 2009. URL <https://papers.nips.cc/paper/3383-spectral-hashing.pdf>.

[47] F. Wu, T. Zhang, A. H. d. Souza Jr, C. Fifty, T. Yu, and K. Q. Weinberger. Simplifying graph convolutional networks. *arXiv preprint arXiv:1902.07153*, 2019.

[48] K. Xu, W. Hu, J. Leskovec, and S. Jegelka. How powerful are graph neural networks? *arXiv preprint arXiv:1810.00826*, 2018.

[49] K. Xu, C. Li, Y. Tian, T. Sonobe, K.-i. Kawarabayashi, and S. Jegelka. Representation learning on graphs with jumping knowledge networks. *arXiv preprint arXiv:1806.03536*, 2018.

[50] N. Yadati, V. Nitin, M. Nimishakavi, P. Yadav, A. Louis, and P. Talukdar. Link prediction in hypergraphs using graph convolutional networks. Manuscript, 2018. URL <https://openreview.net/forum?id=ryeaZhRqFm>.

[51] J. You, R. Ying, and J. Leskovec. Position-aware graph neural networks. *arXiv preprint arXiv:1906.04817*, 2019.

[52] M. Zaheer, S. Kottur, S. Ravanbakhsh, B. Poczos, R. R. Salakhutdinov, and A. J. Smola. Deep sets. In *Advances in neural information processing systems*, pages 3391–3401, 2017.

[53] M. Zhang and Y. Chen. Link prediction based on graph neural networks. In *NeurIPS*, 2018.

Adversarial Permutation Guided Node Representations for Link Prediction (Appendix)

Contents

- In Appendix A we provide a more detailed discussion of prior work.
- In Appendix B we present additional details about our hashing and bucketing methods.
- In Appendix C we give the specifications of all the network modules used in PERMGNN and complete settings of our experiments, which, together with our code, makes our results reproducible.
- In Appendix D we report on additional experiments on PERMGNN, its variations, and other baseline methods.

A Detailed commentary on prior work

Link prediction and GNNs. Unsupervised LP algorithms compute a heuristic confidence score of a potential edge, given a node pair, based solely on local network structures [2, 23]. Adamic-Adar (AA), common-neighbor (CN) and Jaccard coefficient (JC) are examples. Prior to deep learning, conventional supervised learning was successfully used for LP [3, 16, 24].

Recent years have witnessed a surge of interest in modeling and learning latent node features, called node embeddings or representations. These are low dimensional compact vectors, compressed from the high dimensional neighborhood information of the larger graph. In contrast to hand-engineered features, node embeddings are modeled using highly expressive neural networks that are trained using the observable graph structure.

Node2Vec [12], DeepWalk [31] and LINE [42] were among the earliest attempts to fit node embeddings. GCNs [17] and RGCNs [36] soon followed. Wang et al. [45] exploited multi-level graph coarsening in their proposed system called MGNN, which benefits from naturally hierarchical knowledge graphs (KGs). Salha et al. [34] extended the GCN paradigm to directed graphs. Yadati et al. [50] extended GCNs to hypergraphs. Other notable enhancements were proposed as GraphSAGE [13], GAT [43], SEAL [53], GIN [48], JKN [49], and P-GNN [51], *inter alia*.

Neural permutation gadgets. Sinkhorn [39] used iterative row and column scaling as an effective way to impute matrices, given marginal constraints. Cuturi [8] exploited this to solve transportation problems approximately. It was soon realized [26, 30] that row and column scaling transform an arbitrary matrix to a near-permutation matrix, while allowing backpropagation. After the seminal deep sets work of Zaheer et al. [52], several efforts [5, 20, 38, 40, 41] were made to capture dependencies between set elements while retaining order invariance by design [27].

(Supervised) locality-sensitive hashing. LSH was proposed in path-breaking papers by Gionis et al. [11] and Charikar [7]. These were *data-oblivious* hashing protocols. Later, data-driven, supervised hashing approaches [19, 25, 46] were proposed.

B Additional details about proposed hashing method

We form the buckets using the recipe of Gionis et al. [11], summarized here for completeness. Given hash bit positions $1, \dots, H$, we select $J < H$ bit positions uniformly at random, L times. (J, L are chosen based on N and performance targets.) Let these bit indices be $I_1, \dots, I_\ell, \dots, I_L$ and let $g_{u,\ell} = b_u \downarrow_{I_\ell}$ be the hash code of node u , projected to the bit positions I_ℓ . We thus obtain L bitvectors from \mathbf{x}_u , called $g_{u,1}, \dots, g_{u,L} \in \{-1, +1\}^J$, which represents a number in $[0, 2^J - 1]$. There are L hashtables, each with 2^J buckets. Node u is registered in each hashtable once. In hashtable number ℓ , it goes into the bucket numbered $g_{u,\ell}$. Qualitatively, if nodes u and v occupy the same bucket in many of the L hashtables, they are very similar. We score $\{u, v\}$ if they share a bucket in any of the L hashtables.

In practice, we set $J=8$ and $L=10$. The hashing/compression network C_ψ is devised with a single linear layer of dimension (D, H) . We choose the output hashcode dimension (H) to be same as input embedding dimension (D), i.e., 16.

C Additional details on experimental setup

C.1 Design specifications of PERMGNN

Excluding the hashing machinery, PERMGNN has three neural modules: 1. The LSTM aggregator LSTM_θ in Eq. (6). 2. The nonlinear component in the outer layer σ_θ in Eq. (7). 3. The permutation generator network T_ϕ in Eq. (13). In the following, we describe the specifications of these components, beginning with the node features $\{f_u\}$.

Specification of f_\bullet . For Cora and Citeseer datasets, node features $\{f_u\}$ are binary vectors indicating presence/absence of corresponding keywords in the document. For the remaining datasets, we define node features as the one-hot representations of the unique node labels.

Specification of LSTM_θ . Across all experiments we used an LSTM with hidden size 32.

Specification of σ_θ . We design σ_θ (Eq. (7)) with a fully connected single layer feed forward network on top of the LSTM. This outputs the final node embeddings with $\text{dim}(x_\bullet) = 16$.

Specification of T_ϕ . We design T_ϕ (Eq. (13)) using a three layer neural network which consists of one linear, one ReLU and and linear layer, having the latent feature dimension 16. In all cases, we use 10 Sinkhorn Operator iterations, with noise factor 1 and a temperature of 0.5. The output of the permutation network is a doubly stochastic matrix of dimension equal to the maximum node neighborhood size in the input graph.

C.2 Dataset details

We use five datasets for evaluation:

1. **Twitter** [21] is a snapshot of a part of Twitter’s social network.
2. **Google+** [22] is a snapshot of a part of Google-Plus social network.
3. **Citeseer** [10] is a snapshot of citation network.
4. **Cora** [10] is a snapshot of citation network.
5. **PB** [1] is a network of US political blogs.

Table 3 shows some characteristics of the data sets we use. They show a diversity of average degree, diameter, and number of node features.

Dataset	$ V $	$ E $	d_{avg}	Diameter	$\text{dim}(f_\bullet)$	$ Q $
Twitter	193	7790	79.73	4	193	190
Google+	769	22515	57.56	7	769	718
Citeseer	3312	7848	3.74	28	3703	1010
Cora	2708	7986	4.90	19	1433	1470
PB	1222	17936	28.36	8	1222	999

Table 3: Dataset statistics.

C.3 Discussion of evaluation protocols and metrics

As discussed in the main paper, we partition edges and non-edges into training, validation and test folds as follows. Each query in the query node set Q is required to be part of at least one triangle. For each $q \in Q$, in the original graph, we partition its neighbors $\text{nbr}(q)$ and non-neighbors $\text{nbr}(q)$ into training, validation and test folds, where the corresponding node pairs are sampled uniformly at random. In the main paper, these were in the ratio 54:6:40. Here we also present results for the ratio 72:8:20. We disclose the resulting sampled graph induced by the training and validation sets to the LP model. After computing the scores for all potential edges, LP algorithms sort the potential edges in decreasing order of scores. In this context, we note the following differences of our protocol from several prior works [13, 53].

1. Some prior LP models, *e.g.*, SEAL [53] remove a large fraction non-edges in the test set to ensure that the number of edges and non-edges in the test set is roughly equal. In contrast, we do not make any perturbation in the test set, which makes the evaluation more realistic as well as challenging. However, for completeness, we also present a comparative analysis of our method against the competitors by curating the test set to ensure that the number of edges and non-edges is roughly equal.

- Often in prior works [13, 53], the underlying LP algorithm sorts all potential edges \bar{E} by decreasing scores $\{s(u, v) \mid (u, v) \in \bar{E}\}$ to output a single *global* ranked list R . However, in practical applications, no end-user (node) of the network observes the global ranking. Therefore, we assume that each node q (regarded as a ‘query’) is provided a *local* ranking R_q of recommended neighbors-to-be. Recommending friends on Facebook, or movies on Netflix, are better served by this protocol.

We measure the accuracy of an LP method in terms of Mean Average Precision (MAP) and Mean Reciprocal Rank (MRR), computed on the ranked lists of predicted neighbors across all the queries. In particular, we compute:

$$\text{MAP} = \frac{1}{|Q|} \sum_{q \in Q} \text{AP}_q, \quad \text{MRR} = \frac{1}{|Q|} \sum_{q \in Q} \frac{1}{r_q}, \quad (15)$$

where AP_q is the average precision and r_q is the rank of the topmost neighbor of the ranked list for the query node q .

C.4 Hyperparameters and policy parameters

For all training, we impose an early stopping criteria based on validation fold AUC and AP scores. We remember the performance from the latest 100 epochs (the so-called ‘patience’ parameter). If the relative variation in AUC and AP fall before the fraction 10^{-4} , we stop training and roll back to the best model in the patience window.

We train our LP model using the ranking loss defined in Eqn (9) with choices of optimizer, learning rate and margin as summarized in Table 4 for reproducibility.

The hashing network C_ψ is trained according to the loss defined in Eqn. (14), with the hyperparameters α and β set to 0.01 for all datasets. In all cases, we train the network C_ψ using SGD optimizer with learning rate of 0.05.

Dataset	Learning Rate	Margin	Optimizer
Twitter	5×10^{-4}	0.01	Adam
Google+	5×10^{-5}	0.01	SGD
Citeseer	5×10^{-5}	0.1	SGD
Cora	5×10^{-5}	0.1	SGD
PB	5×10^{-6}	0.01	SGD

Table 4: Dataset specific hyperparameters of PERMGNN.

C.5 Infrastructure and implementation details

PERMGNN was implemented using Python 3.6.9 and Torch 1.5.0. It was run on Xeon E5-2620 2.10GHz CPUs plus Titan/Xp GPUs with 12GB RAM. We re-implemented AA and CN, and used the following public implementations for all embedding based link predictors.

- Set Transformer: https://github.com/juho-lee/set_transformer
- GAE (GCN), Gravity: https://github.com/deezer/gravity_graph_autoencoders
- GAT, GIN, GraphSAGE, PGNN: <https://github.com/JiaxuanYou/P-GNN>
- AA/CN: https://networkx.github.io/documentation/networkx-1.10/reference/algorithms.link_prediction.html
- SEAL: <https://github.com/muhanzhang/SEAL>

D Additional experiments

D.1 Comparison with additional baselines

In the main paper, we compared PERMGNN against eight baselines. Here, we compare our method against three additional baselines, *viz.*, PGNN [51], GAT [43] and GIN [48]. Table 5 summarizes the results which show that PERMGNN consistently outperforms these additional baselines across different datasets.

	Mean Average Precision (MAP)					Mean Reciprocal Rank (MRR)				
	Twitter	Google+	Cora	Citeseer	PB	Twitter	Google+	Cora	Citeseer	PB
AA	0.644	0.263	0.318	0.400	0.164	0.839	0.508	0.412	0.455	0.423
CN	0.614	0.234	0.284	0.367	0.134	0.824	0.495	0.369	0.405	0.407
Node2Vec	0.621	0.272	0.369	0.464	0.135	0.838	0.472	0.422	0.515	0.255
DeepWalk	0.581	0.227	0.356	0.449	0.136	0.776	0.403	0.402	0.491	0.248
GCN	0.630	0.287	0.353	0.455	0.142	0.812	0.433	0.397	0.497	0.268
SEAL	0.652	0.376	0.382	0.420	0.302	0.837	0.661	0.486	0.483	0.630
GraphSAGE	0.668	0.244	0.291	0.380	0.109	0.782	0.357	0.307	0.386	0.188
Gravity	0.686	0.326	0.351	0.447	0.158	0.839	0.490	0.398	0.497	0.286
PGNN	0.603	0.176	0.323	0.405	0.107	0.731	0.267	0.365	0.438	0.157
GAT	0.659	0.248	0.303	0.392	0.113	0.745	0.392	0.323	0.425	0.199
GIN	0.660	0.281	0.313	0.402	0.131	0.759	0.424	0.351	0.444	0.220
PERMGNN	0.910	0.630	0.923	0.936	0.425	0.972	0.752	0.939	0.941	0.609

Table 5: MAP and MRR for all LP algorithms including **three additional baselines, viz., PGNN [51], GAT [43] and GIN [48]** on the ranked list of all potential edges across all five datasets, with 40% test set. Numbers in bold font (boxes) indicate the best performer (resp. second best performer). PERMGNN outperforms all the new baselines in all scenarios.

	Mean Average Precision (MAP)					Mean Reciprocal Rank (MRR)				
	Twitter	Google+	Cora	Citeseer	PB	Twitter	Google+	Cora	Citeseer	PB
AA	0.673	0.582	0.601	0.626	0.548	0.856	0.758	0.585	0.629	0.733
CN	0.640	0.554	0.576	0.582	0.518	0.852	0.745	0.537	0.546	0.714
Node2Vec	0.646	0.626	0.673	0.692	0.578	0.847	0.747	0.707	0.739	0.678
DeepWalk	0.611	0.574	0.671	0.680	0.555	0.795	0.687	0.705	0.716	0.654
GCN	0.656	0.622	0.662	0.689	0.572	0.823	0.696	0.696	0.726	0.668
SEAL	0.679	0.692	0.710	0.673	0.737	0.861	0.840	0.767	0.708	0.898
Gravity	0.708	0.660	0.665	0.688	0.564	0.859	0.731	0.693	0.720	0.636
PGNN	0.628	0.460	0.641	0.635	0.487	0.746	0.504	0.666	0.650	0.524
GAT	0.687	0.573	0.607	0.624	0.513	0.758	0.642	0.615	0.656	0.558
GIN	0.681	0.582	0.612	0.634	0.513	0.772	0.645	0.632	0.670	0.550
GraphSAGE	0.691	0.554	0.603	0.611	0.496	0.788	0.617	0.606	0.609	0.535
PERMGNN	0.908	0.918	0.988	0.980	0.892	0.994	0.942	0.990	0.980	0.940

Table 6: MAP and MRR for all LP algorithms including three additional baselines, viz., PGNN [51], GAT [43] and GIN [48] on the ranked list of the potential edges obtained after deleting a fraction of non-edges to maintain balance between number of edges and number of non-edges on the original 40% test set. Numbers in bold font (boxes) indicate the best performer (resp. second best performer). PERMGNN outperforms all the new baselines in all scenarios.

D.2 Effect of changing the ratio of edges to non-edges

As mentioned earlier, some prior LP implementations like SEAL [53] remove a fraction non-edges from the test set to ensure that the number of edges and non-edges in the test set are roughly equal. Here, we use this protocol for evaluation. Table 6 dissects a comparative analysis of our method against the all the competitors, where we curate the 40% test set to roughly balance the number of edges and non-edges. With this artificially balanced test folds, most LP methods apparently gain in MAP and MRR, compared to retaining the complete test set consisting of all potential edges. However, PERMGNN continues to consistently outperform the baselines under this modified evaluation protocol.

D.3 Comparison with richer set aggregators

Next, we compare PERMGNN against an alternative permutation desensitization approach, in which we increase the capacity of GCN aggregator (while keeping it order invariant by design) by explicitly modeling dependencies between neighbors using the *Set-transformer* [20]. Table 7 summarizes the results which show that PERMGNN greatly outperforms Set-transformer in all the datasets, except Twitter, where it loses by a mild margin.

D.4 Stability to training size

Next we analyze the effect of size of training set on the performance of PERMGNN and other competitive baselines. Table 8 summarizes the results which show that 1. the performance of all methods mostly improve with increase in the size of training set; and, 2. PERMGNN outperforms its competitors for both 60% and 80% training size.

Dataset	MAP		MRR	
	PermGNN	Set-transformer	PermGNN	Set-transformer
Twitter	0.911	0.926	0.989	0.997
Google+	0.625	0.364	0.778	0.484
Citeseer	0.973	0.695	0.976	0.737
Cora	0.959	0.721	0.961	0.756
PB	0.551	0.199	0.703	0.484

Table 7: Performance comparison between PERMGNN and a variant of GCN where the aggregator is devised using Set-transformer [20]. Numbers in bold font indicate the best performer. Except for Twitter, PERMGNN outperforms Set-transformer in all the datasets in terms of both MAP and MRR.

Dataset	TS%	MAP				MRR				
		PermGNN	SEAL	Gravity	AA	Node2Vec	PermGNN	SEAL	Gravity	
Twitter	60	0.910	0.652	0.686	0.644	0.621	0.972	0.837	0.839	0.838
	80	0.911	0.703	0.730	0.735	0.692	0.989	0.863	0.854	0.902
Citeseer	60	0.936	0.420	0.447	0.400	0.464	0.941	0.483	0.497	0.455
	80	0.959	0.530	0.465	0.477	0.493	0.961	0.580	0.520	0.534
Gora	60	0.923	0.382	0.351	0.318	0.369	0.939	0.486	0.398	0.412
	80	0.973	0.517	0.401	0.447	0.449	0.976	0.577	0.427	0.521
PB	60	0.425	0.302	0.158	0.164	0.135	0.609	0.630	0.286	0.423
	80	0.551	0.357	0.189	0.270	0.190	0.703	0.640	0.332	0.519
Google+	60	0.630	0.376	0.326	0.263	0.272	0.752	0.661	0.490	0.508
	80	0.625	0.452	0.356	0.341	0.351	0.778	0.719	0.528	0.551

Table 8: Effect of size of training set (TS) on the performance of our model and several competitive baselines. Numbers in bold font indicate the best performer.

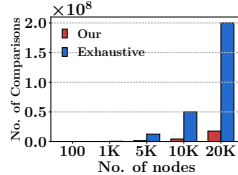


Figure 7: Scalability analysis of our proposed hashing method and the exhaustive enumeration on Barabasi-Albert graphs [4] of roughly same average degree. Our hashing method offers significant gains in terms of reducing the number of comparisons against exhaustive enumeration, across different number of nodes.

D.5 Scalability analysis of our proposed hashing method

Finally, to study asymptotic scalability, we generate Barabasi-Albert graphs [4] of various sizes, having maximum degree 10. We train PERMGNN and then predict top- K neighbors for each node with $K=10$, using both exhaustive comparison and LSH with our binary codes (14). Figure 7 summarizes the results, which shows that our hashing method achieves significant gains in terms of reducing the number of comparisons against exhaustive enumeration of pairwise scores.